XSOL, a Combined Integral Equation (XRISM) and Quantum Mechanical Solvation Model: Free Energies of Hydration and Applications to Solvent Effects on Organic Equilibria

Lei Shao, Hsiang-Ai Yu,† and Jiali Gao*

Department of Chemistry, State University of New York at Buffalo, Buffalo, New York 14260

Received: June 16, 1998; In Final Form: September 4, 1998

A combined XRISM integral equation and quantum mechanical solvation model (XSOL) is presented and tested for the computation of free energies of hydration of organic compounds. The method features the extended reference interaction site model (XRISM) for the description of solute−solvent interactions and a quantum mechanical representation of the solute molecule. A coupled self-consistent-field procedure is used to achieve the convergence of the solvent structural reorganization and the electronic polarization of the solute molecule in solution. The present XSOL model is tested through computation of free energies of hydration of a series of organic compounds and the medium dependence of a number of organic equilibria in solution. The method complements continuum self-consistent reaction field (SCRF) methods and explicit Monte Carlo and molecular dynamics simulations, and it is much more efficient than QM/MM simulation approaches for estimating solvent effects on organic processes in aqueous solution.

Introduction

The combination of quantum mechanics (QM) and classical molecular mechanics (MM) provides an attractive approach for determining molecular structure, energetics, and charge polarization of organic species in solution.[1] Numerous advantages exist with the use of such combined QM/MM methods. The solute molecule is treated by quantum chemical techniques, which can be systematically improved in accuracy,[2] whereas the solvent is treated classically, which is extremely efficient in computational speed. Furthermore, the generality of the method is evident from studies of chemical reactions in solution, where there is no need to specifically parametrize MM potential functions for each new reaction to be investigated. Depending on the representation of the solvent, the coupling between the QM and MM region of a solution system can be achieved in two ways through (1) continuum self-consistent reaction field (SCRF) models[3] and (2) atomistic molecular dynamics and Monte Carlo simulation techniques.[1,4−10] Both approaches have been widely used, and have proven to be remarkably successful in the description of solvent effects on a variety of chemical and biochemical phenomena in aqueous and nonaqueous solutions.[1,3,10]

In the continuum solvation model, the solvent is treated as a dielectric medium using the Poisson equation or the Poisson−Boltzmann equation for nonzero ionic strength. The simplest form of this approach is the Born solvation model for spherical ions.[3] These calculations yield only the electrostatic component of the total solvation free energy, which is often augmented by other contributions, including surface tension and the free energy of cavitation.[3,11] Although computationally efficient, a major drawback of the continuum models is a lack of knowledge of specific solute−solvent interactions. It is sometimes necessary to include one or more explicit solvent molecules to account for specific hydrogen bonds.[12]

In the second approach, solvent molecules are explicitly included in computer simulations in which the intermolecular interactions are typically described by an analytical force field.[13] Solute−solvent electrostatic interactions are incorporated into the Hamiltonian for the "quantum mechanical" solute, leading to the determination of the solute wave function in solution.[1] Although more realistic, the use of an explicit solvent dramatically increases the computational time necessary to carry out sufficient statistical sampling in these simulations. Furthermore, to obtain accurate results for solvation free energies, long-range electrostatic interactions must be treated accurately by moving beyond the spherical cutoff scheme.[13] To this end, long-range electrostatic interactions have recently been incorporated into combined QM/MM simulations through Ewald summation.[14]

An alternative approach to solvation is statistical mechanical integral equation theories of liquids.[15] In particular, the reference interaction site model (RISM) of Chandler and Andersen is extremely successful in providing both qualitative and quantitative insight about solvation.[16,17] The RISM integral equation theory, like molecular dynamics and Monte Carlo simulation, is a microscopic method that provides detailed information about solute−solvent interactions in terms of statistical site−site distribution functions. Yet, like the continuum models, it is computationally efficient, and more importantly, there is no complication of truncating long-range electrostatic interactions as in molecular simulations. Thus, the combination of the RISM integral equation theory and QM methods would complement both continuum and explicit simulation techniques.

Indeed, integration of the RISM model with ab initio Hartree−Fock and multiconfiguration self-consistent field (MCSCF) methods has been reported by Hirata and coworkers.[18,19] In essence, the implementation is analogous to the continuum SCRF procedure.[3] Making use of electrostatic potential (ESP) derived charges, the method has been applied to a number of organic systems, exemplified by the computation

† Present address: Charles River Associates, Inc., Boston, MA.

10.1021/jp982643v CCC: $15.00
Published on Web 11/21/1998

of the free energy difference of alkylamines in water,[19] the acidity difference of haloacetic acid,[18d] and the solvent effect on electronic absorption energies.[18b] However, the method has not been optimized for general, accurate calculations of the absolute free energies of solvation for organic compounds.

In this study, an alternative approach is explored for the coupling between the QM and MM region, with the semiempirical AM1[20] and PM3[21] model chosen for the solute and the RISM[16] integral equation theory for the solvent by making use of Jorgensen's three-site TIP3P model.[22] In particular, the semiempirical wave function is used to obtain atomic charges with the charge model 1 (CM1) algorithm recently developed by Cramer and Truhlar and co-workers.[23] The CM1 charges are determined from a multiparameter scaling procedure that has been parametrized to reproduce experimental dipole moments for neutral molecules in the gas phase.[23] Since the wave function of the solute molecule will be polarized through the QM/MM coupling, the CM1 charges derived from the polarized wave function reflect such condensed-phase polarization effects. The CM1 charges have been employed in the newest versions of the extremely successful generalized Born solvation models (SMX) by these authors[24] and have been chosen by Kaminski and Jorgensen in Monte Carlo simulations.[25]

The aim of the present study is to develop a general procedure for computing the absolute free energies of solvation for organic molecules with an accuracy comparable to that from the continuum SCRF solvation models or free-energy perturbation (FEP) simulations.[3,10,26] The present method is referred to as the XSOL model for the combination of extended RISM (XRISM) and the semiempirical AM1/PM3 solvation model. The computed free energies of hydration for a series of 21 molecules of various functionalities are found to be in good agreement with experiment, employing a small number of adjustable parameters (the Lennard−Jones σ and ϵ for each element). The XSOL model is further tested by the computation of solvent effects on the torsional free-energy profile of 1,2-dichloroethane and the tautomeric equilibria of 2- and 4-hydroxypyridine and pyridone. These applications demonstrate the applicability and limitations of the XSOL model.

Method

A. XRISM Method. The RISM integral equation theory of Chandler and Andersen divides molecules into interaction sites,[16] analogous to the force fields used in fluid simulations. The extended RISM (XRISM) is an extension of the original theory for polar solvents.[17] There are two equations with two unknowns: the total correlation functions, $h(r)$, and the direct correlation functions, $c(r)$, where r is the distance variable. For a system of rigid molecules, in which the solute molecule (x) is dissolved in a solvent (s) at infinite dilution ($\rho_x \rightarrow 0$), the XRISM equations in Fourier k-space (denoted by the caret) for solvent−solvent and solute−solvent interactions are[16,17]

$$\hat{\boldsymbol{h}}_{ss} = \hat{\boldsymbol{w}}_s \hat{\boldsymbol{c}}_{ss} \hat{\boldsymbol{w}}_s + \rho_s \hat{\boldsymbol{w}}_s \hat{\boldsymbol{c}}_{ss} \hat{\boldsymbol{h}}_{ss} \quad (1)$$

$$\hat{\boldsymbol{h}}_{xs} = \hat{\boldsymbol{w}}_x \hat{\boldsymbol{c}}_{xs} \hat{\boldsymbol{w}}_s + \rho_s \hat{\boldsymbol{w}}_x \hat{\boldsymbol{c}}_{xs} \hat{\boldsymbol{h}}_{ss} \quad (2)$$

where $\hat{\boldsymbol{h}}$ and $\hat{\boldsymbol{c}}$ are matrixes of the intermolecular total correlation function and the direct correlation function, respectively, ρ_s is the solvent density, and $\boldsymbol{w}$ is the intramolecular correlation matrix. The element of $\hat{\boldsymbol{w}}$ can be expressed in Fourier representation as $\hat{w}_{\alpha\gamma}(k) = (\sin kR_{\alpha\gamma})/(kR_{\alpha\gamma})$ with $R_{\alpha\gamma}$ being the distance between atoms α and γ.

The second equation is the site−site closure relationship. Although a number of choices are available, the hypernetted chain (HNC) closure has been shown to provide good results for polar and ionic aqueous solutions[27−29] and is adopted in the present XSOL model

$$\boldsymbol{h}_{\alpha s}(r) = e^{-U_{\alpha s}(r)/kT + \boldsymbol{h}_{\alpha s}(r) - c_{\alpha s}(r)} - 1 \quad (3)$$

where the subscript s specifies a solvent site and α either a solute or a solvent site. In eq 3, the site−site intermolecular potential $U_{\alpha s}(r)$ contains a short-range Lennard−Jones term and a long-range electrostatic term. For solvent−solvent interactions, $U_{ss}(r)$ is determined by the TIP3P model for water,[22] which has been slightly modified for use in the XRISM calculations.[28,29] For solute−solvent interactions, the short-range Lennard−Jones terms are written as

$$U_{xs}^{vdW}(r_{xs}) = 4\epsilon_{xs}\left[\left(\frac{\sigma_{xs}}{r_{xs}}\right)^{12} - \left(\frac{\sigma_{xs}}{r_{xs}}\right)^{6}\right] \quad (4)$$

where the parameters σ_{xs} and ϵ_{xs} are determined according to the combining rules such that $\sigma_{xs} = (\sigma_x + \sigma_s)/2$ and $\epsilon_{xs} = (\epsilon_x\epsilon_s)^{1/2}$. The solvent parameters σ_s and ϵ_s are taken from the TIP3P model for water and are kept unchanged. The parameters (σ_x and ϵ_x) of the *solute atoms* are optimized in XSOL calculations to yield the best agreement between computed and experimental solvation free energies. These are the empirical parameters inherently involved in any QM/MM combinations and must be optimized analogously.[1] For long-range interactions, U_{xs}^{el} is determined by the Coulombic term

$$U_{xs}^{el}(r) = \frac{q_x q_s}{r_{xs}} \quad (5)$$

where q_s is the empirical partial charge for a solvent atom and q_x is the CM1 charge for solute atom x, which is derived from the solute wave function.[23] To solve the XRISM equations, a renormalization technique is used for the electrostatic term and the number of Fourier points in the numerical iteration are 512, corresponding to 0.00598 to 164 Å in real space.[17]

B. QM/MM Coupling. Incorporation of electrostatic terms from the XRISM solvent into Hartree−Fock calculations is analogous to combined QM/MM methods used in explicit computer simulations or continuum SCRF solvation models.[1,3,18] This involves a modification of the gas-phase Fock matrix by the electrostatic potential arising from the solvent. In the XSOL model, the solute is treated by the semiempirical Austin model 1 (AM1) and parametrized model 3 (PM3) methods.[20,21] Semiempirical models are chosen in the initial application because they can be applied to large molecular systems.[18] The procedure would complement the popular solvation models (SMX) developed by Cramer and Truhlar, where the AM1 and PM3 models are also used,[3b,24] as well as other approaches.[3a,25,26] Since the overlap integral is unity in the neglect diatomic differential overlap (NDDO)[30] approximation that is used in the AM1 and PM3 model along with the fact that only atomic site−site correlation functions are available from the XRISM calculation, the Fock matrix element for the solute in solution is given by eq 6

$$F_{\mu\mu} = F^{\circ}_{\mu\mu} - \sum_x \delta(\mu\epsilon x) V(\boldsymbol{R}_x) \quad (6)$$

where the basis functions are located on atom x, $F^{\circ}_{\mu\mu}$ is an element of the gas-phase Fock matrix, and $V(\mathbf{R}_x)$ is the electrostatic potential from the solvent at the position of solute atom x. The electrostatic potential, $V(\mathbf{R}_x)$, is evaluated using

the trapezoidal numerical integral scheme from site−site pair distributions

$$V_x(\boldsymbol{R}_x) = 4\pi \int_0^\infty \sum_{s=1}^{S} q_s \rho_s r_{xs} g_{xs}(r_{xs}) \mathrm{d}r_{xs} \quad (7)$$

where $g_{xs}(r_{xs})$ is the radial distribution function between solute atom x and solvent site s and is related to the total correlation function by $g_{xs}(r_{xs}) = h_{xs}(r_{xs}) + 1$.

C. Free Energy of Hydration. In the XSOL model, the free energy of hydration is written as

$$\Delta G_h = \Delta G_{Xs} + \Delta E_{pol} \quad (8)$$

where ΔG_{xs} is the free energy of solvation due to solute−solvent interactions and solvent reorganization and ΔE_{pol} is the change in the electronic energy or polarization of the solute in going from the gas phase into solution. The standard state in the present study corresponds to 1 mol/L ideal gas for the vapor phase and 1 mol/L ideal solution for the solution phase. In eq 8, ΔE_{pol} is defined as follows and is analogous to previous studies[1a,10]

$$\Delta E_{pol} = \langle \Psi | \hat{H}_{eff} | \Psi \rangle - \langle \Psi^\circ | \hat{H}^\circ | \Psi^\circ \rangle \quad (9)$$

where Ψ and Ψ° are the solute wave functions in solution and in the gas phase, respectively. $\hat{H}_{eff}$ is the effective Hamiltonian of the solute molecule in solution, which is obtained by including the solute−solvent interaction terms (eq 7) in the Hamiltonian of an isolated solute in the gas phase ($\hat{H}^o$).[1,3−10,25,26] ΔG_{Xs} is computed using the Chandler−Singh−Richardson equation derived with the assumption of Gaussian fluctuations (GF) for the solvent:[31]

$$\Delta G_{Xs} = -4\pi\rho_s RT \sum_x \sum_s \int_0^\infty r^2 \left[c_{xs}(r) + \frac{1}{2} h_{xs}(r) c_{xs}(r) \right] \mathrm{d}r \quad (10)$$

An alternate formula was also derived by Singer and Chandler for use with the HNC closure.[32] It is found here and in early works that eq 10 gives superior results.[18,19]

D. Computational Details. A coupled iterative scheme is used to solve the coupled XRISM and HF−SCF equations.[18,29,33] Throughout this study, the solute geometry is held rigid at its optimized structure in the gas phase, since previous studies showed that geometry optimizations in solution only have minor corrections to the computed solvation free energy.[3b] The XRISM equations are solved using the method described previously,[17,29] with an initial guess for the solute CM1 charges from the gas-phase wave function. Then the electrostatic potential at the position of the solute atomic sites is determined using the converged total correlation function. The electrostatic potentials are then incorporated into the Fock matrix to yield an updated density matrix for the solute, from which a new set of CM1 charges are enumerated. These charges are used in subsequent XRISM iterations to yield another set of pair correlation functions. This procedure, analogous to the SCRF scheme,[3] is continued until both the electronic energy and the solvent structure become self-consistent with a criterion of charge density change less than 10^{-4} e units between successive coupled XRISM-HF iterations. The semiempirical MOPAC package is used in all electronic structure calculations.[34] Usually it requires several hundred to a thousand iterations to attain the XRISM convergence, which is compounded by about 5−10 cycles of XRISM-HF iteration. Thus, the computational cost is still substantial if ab initio and density-functional methods are used for the solute. Employing semiempirical models, computation of free energies of hydration for typical organic molecules containing less than 15 non-hydrogen atoms takes about 2 h CPU time on a SGI Indigo2/R10000 workstation. For comparison, if hybrid QM/MM free-energy simulations were performed,[1] it would require 2−3 weeks of computer time. The XSOL program is available upon request from the authors.

TABLE 1: Lennard−Jones Parameters for Solute Atoms in the XSOL Model

	AM1		PM3	
atom	σ (Å)	ϵ (kcal/mol)	σ (Å)	ϵ (kcal/mol)
H (C)	1.80	0.02	1.60	0.04
H (heteroatom)	0.50	0.02	0.50	0.05
C	4.40	0.08	4.30	0.10
N	4.40	0.35	3.70	0.70
O (sp^3)	3.55	0.40	3.50	0.35
O (sp^2)	3.55	0.40	3.60	0.30
Cl	4.60	0.60	4.60	0.60

With the choice of the CM1 charges and the potential function parameters for the solvent (TIP3P) kept unchanged,[22,23] the only adjustable parameters in the coupled QM and XRISM integral equation approach are the Lennard−Jones σ_x and ϵ_x values for the solute atom (eq 4). These parameters are determined by an iterative process of trial and error and by comparison of trends of computed solvation free energies with experiment. The same process has been used and described in the development of the SMX parameters[24] as well as the CHARMM[35] and OPLS force fields.[36] For neutral solutes, we found that each element only requires one set of parameters (σ_x and ϵ_x), except hydrogen for which a distinction between hydrogen attached to a carbon or to a non-carbon atom must be made. The final parameters for both AM1 and PM3 models are listed in Table 1.

Results and Discussion

A. Free Energy of Hydration. Solvation free energies for a series of 21 molecules from both the AM1 and PM3 model are listed in Table 2, along with the experimental values. For comparison, the predictions by the SM5.4[24] and the PSGVB−PB[26] continuum solvation models and by Monte Carlo simulations employing scaled CM1 charges for aqueous solution[25] are also included in Table 2. These molecules contain a wide variety of functional groups, including hydrocarbons, alcohols, ethers, carbonyl groups, acids, esters, amines, amides, acetonitrile, and aromatic compounds. Because of the difference in charge polarization between AM1 and PM3, particularly for molecules containing nitrogen, there are noticeable changes in the Lennard−Jones parameters for the two models. Nevertheless, these parameters are reasonably close to those used in empirical force fields for proteins and organic liquids.[35,36]

With the use of a single set of adjustable parameters, in addition to the heuristic choice of the CM1 charges for the solute atoms, the computed free energies of hydration are found to be in good agreement with experimental data.[37] The average errors in computed ΔG_{hyd} from the present XSOL model are 1.1 kcal/mol using both the AM1 and PM3 methods, which cover a range from +2 to −10 kcal/mol in solvation free energy. The error range is similar to results obtained from free-energy perturbation simulations employing the combined QM/MM AM1/TIP3P potential, which yielded an average uncertainty of 1.4 kcal/mol for 10 neutral solutes in water.[6] In another approach using scaled CM1/AM1 charges in Monte Carlo simulations, the average error in computed ΔG_h was 1.1 kcal/mol for 13 solutes.[25] For a similar set of 29 molecules, Tannor et al. obtained an error of 0.6 kcal/mol using the ab initio HF/6-31G**

TABLE 2: Calculated and Experimental Free Energies of Hydration, ΔG_h° (kcal/mol)

	XSOL		SM5.4[a]				
molecule	AM1	PM3	AM1	PM3	PSGVB[b]	MC-AOC[c]	exp[a]
CH_4	4.5	3.5	2.0	2.1			2.0
CH_3CH_3	4.1	2.9	1.2	1.3		2.5	1.9
C_6H_6	−0.7	−1.5	−1.0	−1.1	−0.8	−2.9	−0.8
$C_6H_5CH_3$	−1.7	−2.6	−0.9	−0.9	−0.8		−0.8
CH_3OH	−4.0	−4.1	−5.4	−5.4	−5.2	−4.4	−5.1
CH_3CH_2OH	−5.5	−5.6	−4.9	−4.8	−4.5		−5.0
2-propanol	−4.0	−4.9	−3.8	−4.1	−4.4		−4.8
phenol	−7.5	−7.3	−6.6	−6.4	−5.9		−6.6
H_2O	−7.7	−6.6	−9.5	−8.6	−7.3		−6.3
CH_3OCH_3	−0.5	−0.7	−2.4	−2.2		−2.6	−1.9
CH_3COCH_3	−1.7	−2.8	−4.3	−4.2	−4.5	−3.6	−3.8
CH_3CO_2H	−6.7	−6.3	−6.5	−6.6	−7.3	−7.7	−6.7
$CH_3CO_2CH_3$	−4.1	−4.3	−4.0	−3.9		−4.6	−3.3
CH_3CN	0.8	−4.7	−4.3	−4.5		−5.0	−3.9
CH_3NH_2	−4.4	−4.7	−5.8	−5.1	−4.3	−6.5	−4.6
$CH_3CH_2NH_2$	−3.2	−4.6	−4.7	−4.2	−4.7		−4.5
CH_3CONH_2	−7.2	−11.7	−10.3	−9.8	−11.0	−11.9	−9.7
(Z)-NMA	−10.0	−10.1	−7.8	−8.7	−8.7		−10.1
(E)-NMA	−10.4	−13.5	−7.3	−9.9	−9.0		−10.1
pyridine	−4.5	−7.2	−5.0	−4.9		−5.1	−4.7
4-me-pyridine	−4.8	−7.8	−4.9	−4.6	−5.1		−4.9

[a] Reference 24. [b] Reference 26. [c] Reference 25.

and GVB/6-31G** method coupled with a numerical Poisson−Boltzmann solver.[26] The SM5.4, on the other hand, was developed with a much larger database including 215 neutral solute molecules.[24] The mean unsigned error in the free energy of hydration was 0.50 and 0.44 kcal/mol for the AM1 and PM3 models, respectively.[24] Overall, the accuracy of the present XSOL model is similar to that from free-energy perturbation simulations using combined QM/MM potentials but with only a fraction of the computational costs. Interestingly, results from well-parametrized continuum models enjoy somewhat smaller average errors than the XSOL model and explicit simulations.

The primary sources of error in the computed free energy are from alkanes and nitrogen-containing compounds. The XSOL/AM1 model has the largest computational error for acetonitrile with a calculated value of 0.8 kcal/mol, compared with the experimental value of −3.9 kcal/mol. The same difficulty has also been observed in hybrid QM/MM simulations using the AM1 model.[4] The PM3 model gives a reasonable result for acetonitrile; however, the computed solvation free energies for pyridine, 4-methylpyridine, and (*E*)-*N*-methylacetamide (NMA) are overestimated by 2.5−3.5 kcal/mol. The error for (*E*)-NMA in the XSOL-PM3 model is of concern since experimental results indicate that the cis and trans forms of NMA have similar free energies of hydration.[37c] The origin of this error is the result of an overestimated charge polarization in the (*E*) conformation (Table 3).

The computed ΔG_h, which corresponds to the free-energy change in transferring a molecule from the gas phase into solution, contains two contributing components in the present XSOL model. ΔG_{Xs} is the solvation free energy due to interactions between the solute and solvent molecules along with the solvent reorganization. The second term, ΔE_{pol}, is the polarization energy of the solute electronic structure by the solvent environment. Because the electronic wave function of the solute molecule in solution is distorted from its gas-phase equilibrium, ΔE_{pol} is necessarily positive according to the variational principle. The relative contributions to ΔG_h are listed in Table 3. It is interesting to note that the polarization contribution to the total solvation free energy is relatively large, further demonstrating the importance of a polarization effect in solvation. The magnitude of the ΔE_{pol} term predicted by the XSOL model is somewhat greater than that obtained from discreet combined QM/MM Monte Carlo simulations.[6] It should also be noted that ΔG_{Xs} is not always greater than the ΔE_{pol} term in magnitude because the former contains the solvent reorganization energy.

TABLE 3: Energy Components in Computed Free Energies of Hydration (kcal/mol)

	XSOL-AM1			XSOL-PM3		
molecule	ΔE_{pol}	ΔG_{Xs}	ΔG_h	ΔE_{pol}	ΔG_{Xs}	ΔG_h
CH_4	0.0	4.5	4.5	0.0	3.5	3.5
CH_3CH_3	0.0	4.1	4.1	0.0	2.9	2.9
C_6H_6	1.5	−2.3	−0.7	1.2	−2.7	−1.5
$C_6H_5CH_3$	1.9	−3.5	−1.7	1.4	−4.0	−2.6
CH_3OH	1.7	−5.8	−4.0	1.8	−5.9	−4.1
CH_3CH_2OH	2.5	−8.0	−5.5	2.4	−8.0	−5.6
2-propanol	1.5	−5.6	−4.0	1.6	−6.5	−4.9
phenol	3.6	−11.1	−7.5	2.9	−10.2	−7.3
H_2O	1.8	−9.5	−7.7	1.7	−8.3	−6.6
CH_3OCH_3	1.2	−1.7	−0.5	1.1	−1.8	−0.7
CH_3COCH_3	2.8	−4.6	−1.7	3.1	−5.9	−2.8
CH_3CO_2H	2.0	−8.7	−6.7	1.9	−8.2	−6.3
$CH_3CO_2CH_3$	2.0	−6.1	−4.1	2.1	−6.3	−4.3
CH_3CN	1.3	−0.5	0.8	1.0	−5.7	−4.7
CH_3NH_2	1.0	−5.4	−4.4	1.0	−5.7	−4.7
$CH_3CH_2NH_2$	0.7	−3.9	−3.2	0.8	−5.4	−4.6
CH_3CONH_2	3.7	−10.9	−7.2	6.6	−18.3	−11.7
(Z)-NMA	3.2	−13.2	−10.0	3.5	−13.6	−10.1
(E)-NMA	6.2	−16.6	−10.4	9.7	−23.2	−13.5
pyridine	2.3	−6.8	−4.5	4.1	−11.4	−7.2
4-me-pyridine	2.0	−6.8	−4.8	3.4	−11.2	−7.8

Upon solvation, the solute electronic structure will be polarized through interactions with the solvent and is reflected by enhanced molecular dipole moments and partial charges. The computed molecular dipole moments are given in Table 4. Overall, dipole moments in aqueous solution show an increase of about 30−70% in aqueous solution over the gas-phase values. Although the induced dipoles are somewhat greater than those obtained from explicit simulations, which are increased about 20−40%,[1,6] the trends from the XSOL predictions are consistent with the combined QM/MM results.

An advantage of the XSOL model over continuum solvation methods is that specific solute−solvent interactions may be examined through radial distribution functions (rdfs). This is

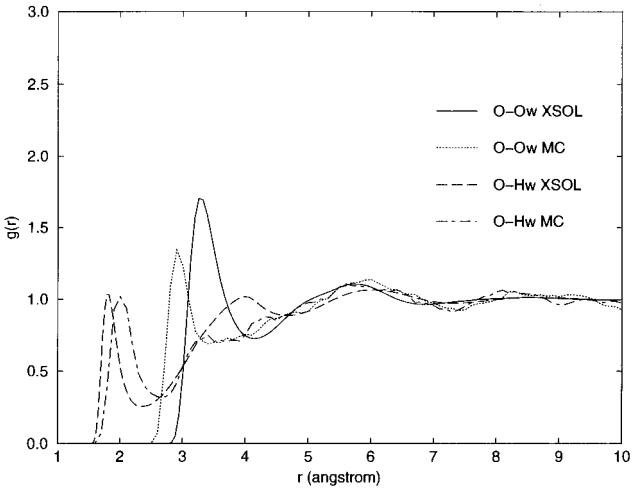

Figure 1. Comparison of the O−O_w and O−H_w radial distributions for acetone in water from the XSOL model and combined QM/MM Monte Carlo simulations.

TABLE 4: Gas-Phase and Aqueous Dipole Moments Calculated Using Charge Model 1 (CM1) and Semiempirical Methods (D)

	CM1-AM1		AM1		CM1-PM3		PM3	
molecule	gas	water	gas	water	gas	water	gas	water
CH_4	0.0	0.0	0.0	0.0	0.0	0.0	0.0	0.0
CH_3CH_3	0.0	0.0	0.0	0.0	0.0	0.0	0.0	0.0
C_6H_6	0.0	0.0	0.0	0.0	0.0	0.0	0.0	0.0
$C_6H_5CH_3$	0.29	0.01	0.26	0.03	0.25	0.02	0.26	0.06
CH_3OH	1.63	2.19	1.62	2.07	1.59	2.21	1.49	1.98
CH_3CH_2OH	1.56	2.43	1.55	2.22	1.56	2.46	1.45	2.14
2-propanol	1.63	2.47	1.69	2.31	1.57	2.47	1.57	2.23
phenol	1.27	2.50	1.24	2.17	1.25	2.46	1.14	2.06
H_2O	2.02	2.35	1.86	2.21	1.92	2.25	1.74	2.09
CH_3OCH_3	1.29	1.89	1.43	1.89	1.17	1.77	1.24	1.68
CH_3COCH_3	2.94	4.66	2.92	4.24	2.92	4.67	2.78	4.11
CH_3CO_2H	1.97	2.62	1.87	2.34	1.97	2.74	1.82	2.42
$CH_3CO_2CH_3$	1.95	3.00	1.74	2.54	2.06	3.21	1.80	2.69
CH_3CN	3.79	4.93	2.89	3.77	3.89	5.78	3.21	4.68
CH_3NH_2	1.40	1.96	1.49	1.77	1.22	1.68	1.40	1.67
$CH_3CH_2NH_2$	1.37	1.88	1.55	1.77	1.14	1.58	1.44	1.68
CH_3CONH_2	3.26	4.95	3.75	5.16	3.68	6.02	3.27	5.16
(Z)-NMA	3.72	5.32	3.81	5.14	3.19	4.87	3.39	4.71
(E)-NMA	2.93	5.36	3.52	5.50	3.72	6.91	3.10	5.58
pyridine	1.54	3.13	1.97	2.90	1.66	3.59	1.94	3.33
4-me-pyridine	1.95	3.24	2.33	3.04	2.00	3.67	2.28	3.46

illustrated by Figure 1, which compares the rdfs for the acetone carbonyl oxygen with water O_w and H_w obtained using the XSOL model and combined AM1/TIP3P Monte Carlo simulations. The position of the first peak in the O−H_w rdf from the XRISM calculation tends to be shorter than the corresponding simulation results, leading to a greater peak height. On the other hand, the O−O_w first peak is shifted outward by about 0.3 Å compared to the simulation data. The discrepancy between XSOL-XRISM and Monte Carlo simulation peaks is due to different van der Waals parameters that have been used in the two calculations. A better agreement would have been obtained if the same parameters were used. A possible approach to reduce the difference in van der Waals parameters is to use the three-dimensional formulation of the RISM equations derived by Cortis et al.[46] The second small peak in the O−H_w at about 4.0 Å may be assigned to the second hydrogen on the water donating a hydrogen bond to the carbonyl oxygen. Overall, the XSOL rdfs show more structured features in the pair distribution functions than the simulation results. The peaks at a distance of about 6 Å, corresponding to the second solvation layer around acetone, are clearly reflected by both the XSOL and simulation methods.

TABLE 5: Calculated Free Energies of Hydration (kcal/mol) and Dipole Moments (D) for Methylated Amines and Ammonia Using the AM1 and PM3 XSOL Model

	μ(gas)[a]	μ(aq)[a]	ΔE_{pol}	ΔG_{Xs}	ΔG_h	exp
			XSOL-AM1			
NH_3	1.76	2.13	0.7	−4.9	−4.2	−4.3
CH_3NH_2	1.40	1.96	1.0	−5.4	−4.4	−4.6
$(CH_3)_2NH$	1.09	1.76	1.3	−5.8	−4.5	−4.3
$(CH_3)_3N$	0.82	1.39	0.7	−4.7	−4.0	−3.2
			XSOL-PM3			
NH_3	1.40	1.61	0.6	−5.2	−4.6	−4.3
CH_3NH_2	1.22	1.68	1.0	−5.7	−4.7	−4.6
$(CH_3)_2NH$	0.97	1.71	1.5	−6.1	−4.6	−4.3
$(CH_3)_3N$	0.56	0.92	0.8	−4.2	−3.3	−3.2

[a] Computed using CM1 charges. The semiempirical dipole moments follow the same trends, and thus, they are not listed here.

In the following, the performance and limitations of the XSOL model are further tested on a number of chemical equilibria in aqueous solution. These systems have been investigated previously by a variety of computational methods including combined QM/MM simulations. The effects of solvation on these molecules are well-established, providing an excellent source of data for comparison. We note that Kaminski and Jorgensen recently described a method making use of scaled CM1 gas-phase charges in Monte Carlo simulations.[25] A similar set of test cases were used by these authors.

B. Free Energy of Hydration of Methylated Amines. The free energies of hydration for methylated amines have been investigated by a number of groups,[38−41] employing a variety of computational methods. An interesting feature in the trend of the experimental free energies of hydration is that there is an initial decrease in free energy with the addition of the first methyl group, which contradicts conventional chemical intuitions in that a methyl group is expected to be hydrophobic.[38] Free-energy perturbation simulations employing effective pair potentials uniformly predict an increase of about 1−2 kcal/mol upon each methyl substitution,[39] although use of polarizable potential functions slightly attenuate the discrepancy,[40,41] suggesting the importance of the polarization effect on this problem. The XSOL/AM1 model gives a reasonable agreement with experiment both in the trend and in the calculated absolute free energy of hydration for this series (Table 5). In Table 5, the computed dipole moments show a trend of decreasing value from ammonia to trimethylamine both in aqueous solution and in the gas phase. The slight decrease (more negative) in the free energy of hydration upon the first and second methyl substitution is echoed by the greater polarization energies for $(CH_3)_2NH$ and CH_3NH_2 than NH_3, which may be attributed to the observed trend. As the third methyl group is added, hydrophobic effects become predominant, which overwhelm the polarization contribution. Similar trends have been obtained by Hirata et al. with their coupled RISM-SCF approach at the HF/6-31G* level; however, the absolute free energies of hydration were not given in that study.[18] The XSOL/PM3 model exhibits similar features as the AM1 method in the correlation of the computed solvation free energies and polarization effect. However, in this case, dimethylamine is predicted to be slightly less solvated than methylamine, in agreement with experiment. Further, the aqueous dipole moments from XSOL/PM3 calculations show a slight increase from ammonia to dimethylamine, in contrast to the XSOL/AM1 results.

Figure 2 depicts the amine N and water O_w rdfs for the these four compounds. It is interesting to observe four isobestic points

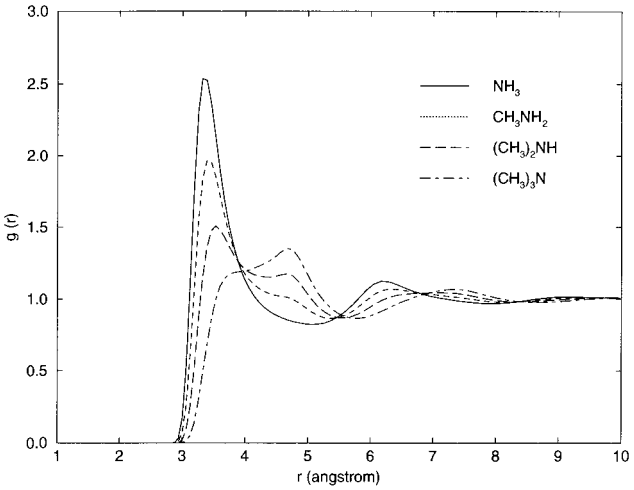

Figure 2. Computed amine N and water O ($N-O_w$) radial distribution functions for NH_3, CH_3NH_2, $(CH_3)_2NH$, and $(CH_3)_3N$ in water.

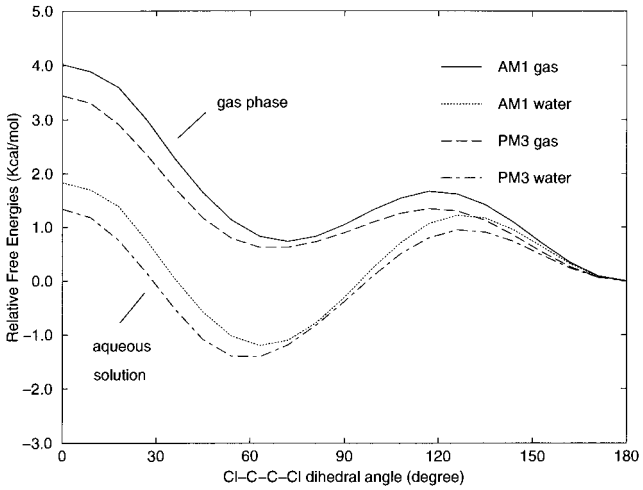

Figure 3. Computed free-energy profile for 1,2-dichloroethane in water from XSOL-AM1 and XSOL-PM3 calculations.

in the rdfs, which reflect the gradual change of solvation shells in going from hydrogen-bonding interactions in NH_3 to primarily hydrophobic interactions in $N(CH_3)_3$. Hydrogen-bonding interactions between the amino group and water are clearly reflected by the first peaks in the rdfs, which gradually diminish upon successive methyl substitutions. Concomitantly, a new peak arises at 4.7 Å, reflecting the first solvation layer of water molecules around the methyl groups at longer distances.

C. Torsional Free-Energy Profile for 1,2-Dichloroethane. The conformational equilibrium of 1,2-dichloroethane provides a classical example of solvent effects on conformational changes of organic compound, and it has been the subject of numerous experimental and computational studies.[25,42] In the gas phase and nonpolar solvent such as cyclohexane, the trans conformation is more stable than the gauche form in free energy by 1.20 and 0.51 kcal/mol, respectively.[42a] As the polarity of the solvent increases, the gauche conformation becomes more populated since its molecular dipole moment changes from zero in the trans conformer to about 3.5 D in the gauche form.[42] Experimentally, the solvent effect was found to stabilize the gauche conformation by −1.42 kcal/mol in going from the gas phase to acetonitrile.[42a] The effect would be expected to be even greater in aqueous solution.

The Lennard−Jones parameters for the chlorine atom are calibrated by comparing the computed and experimental free energies of hydration for CH_3Cl, CH_2Cl_2, and $CHCl_3$. With the parameters listed in Table 1, the computed ΔG_h are 1.9, −0.4, and −1.4 kcal/mol for these three compounds, respectively, which may be compared with the experimental values (−0.6, −1.4, and −1.1 kcal/mol).

The computed free-energy profiles as a function of the dihedral angle around the central C−C bond are shown in Figure 3, using both the XSOL/AM1 and XSOL/PM3 model. The differences in the free energy of hydration between the gauche and trans form are listed in Table 6. For 1,2,-dichloroethane, the XSOL calculations yield a solvent effect of −1.94 kcal/mol at the AM1 level and −2.03 kcal/mol using the PM3 method, in favor of the gauche conformer. This is accompanied by a shift in the minimum of the gauche conformation from 72° (70°) in the gas phase using the AM1 (PM3) model to 63° (60°) in water. For comparison, using the Monte Carlo free-energy perturbation method along with the scaled CM1 charges, Kaminski and Jorgensen found that the trans-gauche relative stability of 1,2-dichloroethane is reversed with a computed solvent effect of −1.19 and −1.48 kcal/mol in acetonitrile and water, respectively.[25] Since the solvent effect in acetonitrile is slightly underestimated by the Monte Carlo simulations, the XSOL results appear to be consistent with the aqueous results of Kaminski and Jorgensen.[25]

TABLE 6: Free Energy Differences (kcal/mol) between the Gauche and Trans Conformers of 1,2-Dichloroethane

				XSOL	
medium	exp[a]	MC-AOC[b]	OPLS-AA[c]	AM1	PM3
gas phase	1.2	0.86	1.17	0.74	0.63
acetonitrile	−0.22	−0.33	−0.33		
aqueous		−0.62		−1.20	−1.40

[a] Reference 42a. [b] Reference 25. [c] Reference 42c.

D. Tautomeric Equilibria in 2- and 4-Hydroxypyridine and Pyridone. Another well-known example having significant solvent effects on chemical equilibria is the tautomeric equilibria of 2- and 4-hydroxypyridine and pyridone.[43] In the gas phase, the hydroxy form is preferred over the lactam form, whereas the two tautomers exist in comparable amounts in chloroform and cyclohexane.[43,44] In aqueous solution, the equilibria is

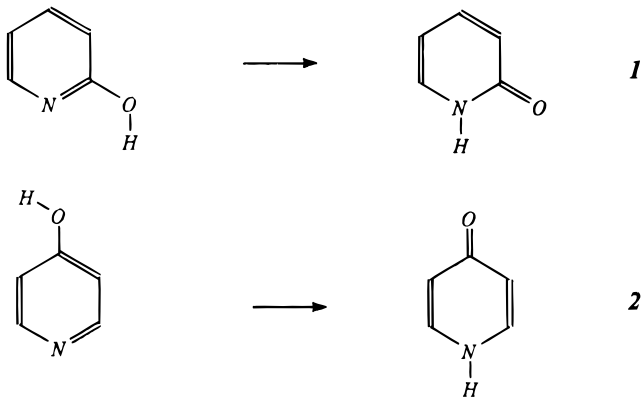

completely shifted to the lactam form due to increased hydrogen-bonding and dipolar interactions.

Table 7 summarizes the computed differences in free energy of hydration for the tautomeric equilibria of 2-hydroxypyridine → 2-pyridone (**1**) and 4-hydroxypyridine → 4-pyridone (**2**) in water. Experimental and early computational results are also listed in Table 7 for comparison.[45] The XSOL/PM3 predictions are found to be in good accord with experiment, with a calculated solvent effect of −4.4 kcal/mol for 2-hydroxypyridine

TABLE 7: Differences in Free Energy of Hydration (kcal/mol) for the Tautomeric Equilibria of 2- and 4-Hydroxypyridine in Water

method	2-HO-pyridine → Pyridone	4-HO-pyridine → pyridone
experiment	-4.6 ± 0.8	<-5.8
MC QM/MM[a]	-5.7 ± 0.2	-7.4 ± 0.2
MC AOC[b]	-2.2 ± 0.2	
AM1-SM2[c]	−2.6	
SCRF[d]	−5.8	
XSOL-AM1	−3.9	−7.0
XSOL-PM3	−4.4	−7.9

[a] Reference 45a. [b] Reference 25. [c] Reference 45b. [d] Reference 45c.

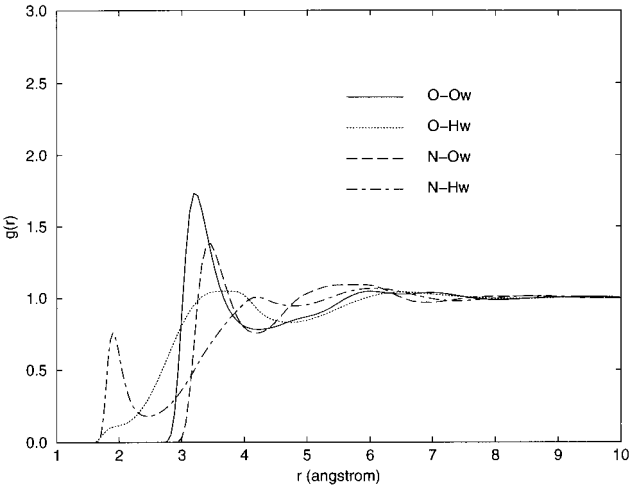

Figure 4. Computed radial distribution functions for 2-hydroxypyridine using XSOL-AM1.

and −7.9 kcal/mol for 4-hydroxypyridine. The results from XSOL/AM1 calculations are also good with predicted solvent effects of −3.9 and −7.0 kcal/mol. Previous Monte Carlo QM/MM simulations employing the AM1 method yielded solvent effects of −5.7 and −7.4 kcal/mol for these two systems, respectively.[45a] Kaminiski and Jorgensen obtained a solvent effect of −2.2 kcal/mol for the 2-hydroxypyridine → 2-pyridone conversion in water. Using the 6-31G* EPS charges and geometries, these authors found that the predicted $\Delta\Delta G_{hyd}$ in water is −6.4 kcal/mol, which lends some insight about the range of uncertainties involved in empirical potential functions for fluid simulations.[25]

Details of hydrogen-bonding interactions are revealed by the computed rdfs for the two systems. Figures 4 and 5 illustrate the change in hydrogen-bonding patterns for 2-pyridone and 2-hydroxypyridine. Hydrogen-bonding interactions between the nitrogen and water hydrogen are clearly reflected by the striking first peak at 1.7 Å in the N−H_w rdf for 2-hydroxypyridine (Figure 4). Integration to the minimum revealed that one water molecule is strongly hydrogen-bonded to the nitrogen. This peak disappears in the N−H_w rdf for 2-pyridone (Figure 5) because the nitrogen is attached to a hydrogen and is now a hydrogen-bond donor. The hydroxy group in 2-hydroxypyridine can potentially form two hydrogen bonds, one donor and one acceptor. However, the acceptor hydrogen bond is weak with an average of 0.3 nearest neighbors. The carbonyl oxygen in 2-pyridone is an excellent hydrogen-bond acceptor, as demonstrated by the first peak in the O−H_w rdf in Figure 5. Integration of the first peak shows that the carbonyl oxygen participate in two hydrogen bonds with the solvent. These findings are in good accord with the results from our previous Monte Carlo simulations employing a combined AM1/TIP3P potential.[45a]

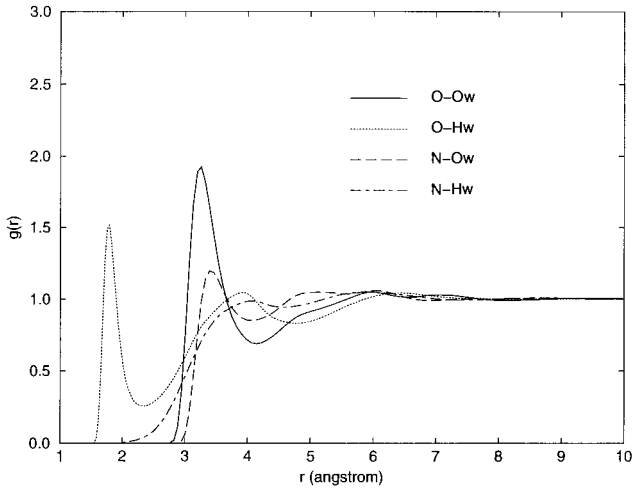

Figure 5. Computed radial distribution functions for 2-pyridone using XSOL-AM1.

Conclusions

A combined integral equation and quantum mechanical solvation model (XSOL) has been presented and tested on the computation of free energies of hydration of a series of organic compounds and on medium effects for organic equilibria in aqueous solution. In the XSOL model, the solute molecules are represented by the semiempirical AM1 or PM3 model and the solvent is approximated by the three-site TIP3P model for water. The solvation process and reorganization of the solvent structures are determined by the extended reference interaction site model (XRISM), which is extremely successful and has been applied to numerous systems. The electronic structure calculations, which yield the solute atomic charges in solution, are performed with the inclusion of the solvent electrostatic potential enumerated from the site−site correlation functions. A key feature of the present method is the use of the charge model (CM1) recently developed by Cramer and Truhlar and co-workers for their solvation models. The method is tested through computation of free energies of hydration for a series of organic molecules and solvent effects on organic equilibria. The unassigned errors are about 1 kcal/mol in comparison with experimental solvation free energies. This is comparable to errors from explicit free-energy perturbation simulations employing either combined QM/MM or empirical potential functions. However, the XSOL model is much more efficient in computational time and complements continuum solvation models and explicit QM/MM simulations. The present RISM integral equation calculations are based on a one-dimensional reduction of the Ornstein−Zernicke equation. Recently, three-dimensional formalisms have been derived in the framework similar to the RISM equations by averaging the orientations of only one of the molecular pair in a correlation function.[46] Thus, the full orientational information can be obtained for the reference solute molecule. It has been shown that the computed pair distribution functions are in better agreement with simulation results than those obtained using the original XRISM equations.[46] There is tremendous opportunity to further improve the accuracy of the present XSOL model by incorporating these new theoretical developments.

Acknowledgment. This research was supported by the National Science Foundation and the National Institutes of Health.

References and Notes

(1) (a) Gao, J. In *Reviews in Computational Chemistry*; Lipkowitz, K. B., Boyd, D. B., Eds.; VCH: New York, 1995; Vol. 7, pp 119−185. (b) Warshel, A. *Computer Modeling of Chemical Reactions in Enzymes and in Solutions*; Wiley: New York, 1991.

(2) Gao, J.; Furlani, T. R. *IEEE Comput. Sci. Eng.* **1995**, 24.

(3) For recent reviews, see: (a) Tomasi, J. *Chem. Rev.* **1994**, *94*, 2027. (b) Cramer, C. J.; Truhlar, D. G. in *Reviews in Computational Chemistry*; Lipkowitz, K. B., Boyd, D. B., Eds.; VCH: New York, 1995; Vol. 6, pp 1−72.

(4) (a) Warshel, A.; Levitt, M. *J. Mol. Biol.* **1976**, *103*, 227. (b) Åqvist, J.; Warshel, A. *Chem. Rev.* **1993**, *93*, 2523. (c) Singh, U. C.; Kollman, P. A. *J. Comput. Chem.* **1986**, *7*, 718. (d) Tapia, O.; Colonna, F.; Angyan, J. G. *J. Chim. Phys.* **1990**, *87*, 875.

(5) Field, M. J.; Bash, P. A.; Karplus, M. *J. Comput. Chem.* **1990**, *11*, 700.

(6) (a) Gao, J.; Xia, X. *Science* **1992**, *258*, 631. (b) Gao, J. *J. Phys. Chem.* **1992**, *96*, 537.

(7) (a) Waszkowycz, B.; Hillier, I. H.; Gensmantel, N.; Payling, D. W. *J. Chem. Soc., Perkin Trans. 2* **1991**, 225, 1819, 2025. (b) Liu, H.; Shi, Y. *J. Comput. Chem.* **1994**, *15*, 1311. (c) Hartsough, D. S.; Merz, K. M., Jr. *J. Phys. Chem.* **1995**, *99*, 384. (d) Thompson, M. A.; Schenter, G. K. *J. Phys. Chem.* **1995**, *99*, 6374. (e) Chatfield, D. C.; Brooks, B. R. *J. Am. Chem. Soc.* **1995**, *117*, 5561. (f) Bakowies, D.; Thiel, W. *J. Phys. Chem.* **1996**, *100*, 10580. (g) Mulholland, A. J.; Richards, W. G. *Protein* **1997**, *27*, 9.

(8) (a) Thery, V.; Rinaldi, D.; Rivail, J.-L.; Maigret, B.; Ferenczy, G. G. *J. Comput. Chem.* **1994**, *15*, 269. (b) Monard, G.; Loos, M.; Thery, V.; Baka, K.; Rivail, J.-L. *Int. J. Quantum Chem.* **1996**, *58*, 153. (c) Gorb, L. G.; Rivail, J.-L.; Thery, V.; Rinaldi, D. *Int. J. Quantum Chem., Quantum Chem. Symp.* **1996**, *30*, 1525. (d) Assfeld, X.; Rivail, J.-L. *Chem. Phys. Lett.* **1996**, *263*, 100.

(9) Maseras, F.; Morokuma, K. *J. Comput. Chem.* **1995**, *16*, 1170.

(10) Gao, J. *Acc. Chem. Res.* **1996**, *29*, 298.

(11) See, for example: (a) Cramer, C. J.; Truhlar, D. G. *Chem. Phys. Lett.* **1992**, *198*, 74. (b) Cramer, C. J.; Truhlar, D. G. *J. Comput.-Aided Mol. Des.* **1992**, *6*, 629. (c) Orozco, M.; Luque, F. J. *Biopolymers* **1993**, *33*, 1851.

(12) Karelson, M.; Zerner, M. C. *J. Am. Chem. Soc.* **1990**, *112*, 9405.

(13) Allen, M. P.; Tildesley, D. J. *Computer Simulations of Liquids*; Oxford University Press: London, 1987.

(14) Gao, J.; Alhambra, C. *J. Chem. Phys.* **1997**, *107*, 1212.

(15) Hansen, J.-P.; McDonald, I. R. *Theory of Simple Liquids*; Academic Press: London, 1986.

(16) (a) Andersen, H. C.; Chandler, D. *J. Chem. Phys.* **1972**, *57*, 1918. (b) Chandler, D.; Andersen, H. C. *J. Chem. Phys.* **1972**, *57*, 1930.

(17) (a) Hirata, F.; Rossky, P. J. *Chem. Phys. Lett.* **1981**, *83*, 329. (b) Hirata, F.; Rossky, P. J.; Pettitt, B. M. *J. Chem. Phys.* **1983**, *78*, 4133.

(18) (a) Ten-no, S.; Hirata, F.; Kato, S. *Chem. Phys. Lett.* **1993**, *214*, 391. (b) Ten-no, S.; Hirata, F.; Kato, S. *J. Chem. Phys.* **1994**, *100*, 7443. (c) Kawata, M.; Ten-no, S.; Kato, S.; Hirata, F. *Chem. Phys.* **1995**, *240*, 199. (d) Kawata, M.; Ten-no, S.; Kato, S.; Hirata, F. *J. Phys. Chem.* **1996**, *100*, 1111. (e) Kinoshita, M.; Okamoto, Y.; Hirata, F. *J. Comput. Chem.* **1997**, *18*, 1320. (f) Akiyama, R.; Hirata, F. *J. Chem. Phys.* **1998**, *108*, 4904.

(19) (a) Kawata, M.; Ten-no, S.; Kato, S.; Hirata, F. *J. Am. Chem. Soc.* **1995**, *117*, 1638. (b) Kawata, M.; Ten-no, S.; Kato, S.; Hirata, F. *Chem. Phys.* **1996**, *203*, 53.

(20) Dewar, M. J. S.; Zoebisch, E. G.; Healy, E. F.; Stewart, J. J. P. *J. Am. Chem. Soc.* **1985**, *107*, 3902.

(21) Stewart, J. J. P. *J. Comput. Chem.* **1989**, *10*, 209, 221.

(22) Jorgensen, W. L.; Chandrasekhar, J.; Madura, J. D.; Impey, R. W.; Klein, M. L. *J. Chem. Phys.* **1983**, *79*, 926.

(23) Storer, J. W.; Giesen, D. J.; Cramer, C. J.; Truhlar, D. G. *J. Comput.-Aided Mol. Des.* **1995**, *9*, 87.

(24) Chambers, C. C.; Hawkins, G. D.; Cramer, C. J.; Truhlar, D. C. *J. Phys. Chem.* **1996**, *100*, 16385.

(25) Kaminski, G. A.; Jorgensen, W. L. *J. Phys. Chem. B* **1998**, *102*, 1787.

(26) Tannor, D. J.; Marten, B.; Murphy, R.; Friesner, R. A.; Sitkoff, D.; Nicholls, A.; Ringnalda, M.; Goddard, W. A.; Honig, B. *J. Am. Chem. Soc.* **1994**, *116*, 11875.

(27) Morita, T. *Prog. Theor. Phys.* **1960**, *23*, 829.

(28) (a) Hirata, F.; Pettitt, B. M.; Rossky, P. J. *J. Chem. Phys.* **1982**, *77*, 509.(b) Chiles, R. A.; Rossky, P. J. *J. Am. Chem. Soc.* **1984**, *106*, 6867. (c) Ichiye, T.; Chandler, D. *J. Phys. Chem.* **1988**, *92*, 5257. (d) Kusalik, P. G.; Patey, G. N. *J. Chem. Phys.* **1988**, *88*, 7715.

(29) (a) Yu, H.-A.; Karplus, M. *J. Chem. Phys.* **1989**, *89*, 2366. (b) Yu, H.-A.; Roux, B.; Karplus, M. *J. Chem. Phys.* **1990**, *92*, 5020. (c) Yu, H.-A.; Karplus, M. *J. Am. Chem. Soc.* **1991**, *113*, 2425.

(30) Pople, J. A.; Santry, D. P.; Segal, G. A. *J. Chem. Phys.* **1965**, *43*, S129.

(31) Chandler, D.; Singh, Y.; Richardson, D. *J. Chem. Phys.* **1984**, *81*, 1975.

(32) Singer, S. J.; Chandler, D. *Mol. Phys.* **1985**, *55*, 621.

(33) Hirata, F.; Levy, R. M. *Chem. Phys. Lett.* **1987**, *139*, 108.

(34) Stewart, J. J. P. *J. Comput.-Aided Mol Des.* **1986**, *4*, 1. Stewart, J. J. P. *MOPAC*; Quantum Chemistry Program Exchange 455, Vol. 6, No. 391, 1986.

(35) (a) MacKerell, A. D.; Bashford, D.; Bellot, M.; Dunbrack, R. L.; Evanseck, J.; Field, M . J.; Fischer, S.; Gao, J.; Guo, H.; Ha, S.; Joseph, D.; Kuchnir, L.; Kuczera, K.; Lau, F. T. K.; Mattos, C.; Michnick, S.; Ngo, T.; Nguyen, D. T.; Prodhom, B.; Roux, B.; Schlenkrich, M.; Smith, J. C.; Stote, R.; Straub, J.; Watanabe, M.; Wiorkievicz-Kuczera, J.; Yin, D.; Karplus, M. *J. Phys. Chem. B* **1998**, *102*, 3586. (b) Brooks, B. R.; Bruccoleri, R. E.; Olafson, B. D.; States, D. J.; Swaminathan, S.; Karplus, M. *J. Comput. Chem.* **1983**, *4*, 187.

(36) Jorgensen, W. L.; Tirado-Rives, J. *J. Am. Chem. Soc.* **1988**, *110*, 1657.

(37) (a) Hine, J.; Mookerjee, P. K. *J. Org. Chem.* **1975**, *40*, 292. (b) Ben-Naim, A.; Marcus, Y. *J. Chem. Phys.* **1984**, *81*, 2016. (c) Wolfenden, R.; Liang, Y.-L.; Matthews, M.; Williams, R. *J. Am. Chem. Soc.* **1987**, *109*, 463.

(38) (a) Ben-Naim, A.; Marcus, Y. *J. Chem. Phys.* **1984**, *81*, 2016. (b) Jones, F. M.; Arnett, E. M. *Prog. Phys. Org. Chem.* **1974**, *11*, 263.

(39) (a) Rao, B. G.; Singh, U. C. *J. Am. Chem. Soc.* **1989**, *111*, 3125. (b) Orozco, M.; Jorgensen, W. L.; Luque, F. J. *J. Comput. Chem.* **1993**, *14*, 1498. (c) Morgantini, P.-Y.; Kollman, P. A. *J. Am. Chem. Soc.* **1995**, *117*, 6057.

(40) (a) Ding, Y.; Bernardo, D. N.; Krogh-Jespersen, K.; Levy, R. M. *J. Phys. Chem.* **1995**, *99*, 11575. (b) Meng, E. C.; Caldwell, J. W.; Kollman, P. A. *J. Phys. Chem.* **1996**, *100*, 2367.

(41) Sitkoff, D.; Sharp, K. A.; Honig, B. *J. Phys. Chem.* **1994**, *98*, 1978. (b) Marten, B.; Kim, K.; Cortis, C.; Friesner, R. A.; Murphy, R. B.; Ringnalda, M. N.; Sitkoff, D.; Honig, B. *J. Phys. Chem.* **1996**, *100*, 11775.

(42) (a) Wiberg, K. B.; Keith, T. A.; Frisch, M. J.; Murcko, M. *J. Phys. Chem.* **1995**, *99*, 9072. (b) Wong, M. W.; Frisch, M. J.; Wiberg, K. B. *J. Am. Chem. Soc.* **1991**, *113*, 4776. (c) Jorgensen, W. L.; McDonald, N. A.; Selmi, M.; Rablen, P. R. *J. Am. Chem. Soc.* **1995**, *117*, 11809.

(43) Reichardt, C. *Solvents and Solvent Effects in Organic Chemistry*; VCH: New York, 1990.

(44) (a) Beak, P.; Fry, F. S. *J. Am. Chem. Soc.* **1973**, *95*, 1700. (b) Frank, J.; Katrizky, A. R. *J. Chem. Soc., Perkin Trans. 2* **1976**, 1428. (c) Albert, A.; Phillips, J. N. *J. Chem. Soc.* **1956**, 1294. (d) Katritzky, A. R. *Handbook of Heterocyclic Chemistry*; Pergamon: Oxford, 1985.

(45) (a) Gao, J.; Shao, L. *J. Phys. Chem.* **1994**, *98*, 13772. (b) Cramer, C. J.; Truhlar, D. G. *J. Comput.-Aided Mol. Des.* **1992**, *6*, 629. (c) Young, P.; Green, D. V. S.; Hillier, I. H.; Burton, N. A. *Mol. Phys.* **1993**, *80*, 503. (d) Wang, J.; Boyd, R. J. *J. Phys. Chem.* **1996**, *100*, 16141.

(46) (a) Cortis, C. M.; Rossky, P. J.; Friesner, R. A. *J. Chem. Phys.* **1997**, *107*, 6400. (b) Beglov, D.; Roux, B. *J. Chem. Phys.* **1996**, *104*, 8678. (c) Beglov, D.; Roux, B. *J. Chem. Phys.* **1995**, *103*, 360. (d) Ikeguchi, M.; Doi, J. *J. Chem. Phys.* **1995**, *103*, 5011.